

## Deformation Trends Among Nuclei with $24 \leq A \leq 30$ : The ( $^3\text{He}, p$ ) and ( $^3\text{He}, p\gamma$ ) Reactions on $^{24}\text{Mg}$ , $^{26}\text{Mg}$ , and $^{28}\text{Si}^\dagger$

B. Lawergren

*Hunter College of the City University of New York, 695 Park Avenue, New York, New York 10021*

and

J. Beyea

*Holy Cross College, Worcester, Massachusetts 01610*

(Received 26 June 1972)

The absolute differential cross sections of the ( $^3\text{He}, p$ ) reactions on  $^{24}\text{Mg}$ ,  $^{26}\text{Mg}$ , and  $^{28}\text{Si}$  have been measured at  $E_{\text{He}} = 10$  MeV. The cross sections to various excited states are in reasonable agreement with rotational-model calculations except for a normalization factor which is different for each target nucleus. The evidence for rotational motion in  $^{26,28}\text{Al}$  and  $^{30}\text{P}$  is reviewed, and the differences in normalization factors are attributed to core overlap differences. In particular, the reduced yield in the  $^{26}\text{Mg}(^3\text{He}, p)^{28}\text{Al}$  reaction reflects a large change in deformation between  $^{26}\text{Mg}$  and  $^{28}\text{Al}$ . In order to determine  $J^\pi$  values in  $^{28}\text{Al}$ ,  $\gamma$ -ray spectra were measured in coincidence with proton groups leading the certain high-lying states in  $^{28}\text{Al}$ . A spin of  $J^\pi = 1^+$  was established for a state at 3.105 MeV in  $^{28}\text{Al}$ .

### 1. INTRODUCTION

The differential cross section for direct two-nucleon transfer (2NT) reactions can be written<sup>1</sup>

$$\frac{d\sigma_{\text{calculated}}}{d\Omega} = \sum^{LSJT} \left| \sum^{l_1 l_2} \mathcal{L}^{1/2}(l_1 l_2; LSJT) B^L(\theta, E, Q) \right|^2 \quad (1)$$

(here  $L, S, J, T$  have the conventional meaning with reference to the two-nucleon cluster while  $l$  specifies the shell-model angular momentum of each individual nucleon).  $\mathcal{L}(l_1 l_2; LSJT)$  is the spectroscopic factor.  $B^L(\theta, E, Q)$  depends on the reaction mechanism only and can be calculated using the distorted-wave Born approximation (DWBA) theory. There are normally many terms in the squared sum making it impossible to solve for a specific  $\mathcal{L}(l_1 l_2; LSJT)$  factor. In one-nucleon transfer (SNT) reactions on the other hand, the spectroscopic factor  $\mathcal{L}(lj)$  can be normally extracted from experiments, since<sup>1</sup>

$$\frac{d\sigma_{\text{calculated}}}{d\Omega} = \sum^{lj} \mathcal{L}(lj) |B^L(\theta, E, Q)|^2. \quad (2)$$

In 2NT reactions  $\mathcal{L}^{1/2}(l_1 l_2; LSJT)$  is generally derived from some model and the absolute (or more commonly, the *relative*) differential cross section is used merely to confirm or reject the model. This, together with the difficulties of computing  $B(\theta, E, Q)$  with present day techniques, has made 2NT reactions less useful for nuclear-structure research than SNT reactions.

We have attempted to circumvent some of these difficulties with 2NT reactions by using a comparative measuring technique:

(i) The absolute differential cross sections were measured for transitions with  $L=0$  or  $L=2$  to all (usually 5 or 6) states below 2 MeV excitation for each of the product nuclei in the series of reactions  $^{24}\text{Mg}(^3\text{He}, p)^{26}\text{Al}$ ,  $^{26}\text{Mg}(^3\text{He}, p)^{28}\text{Al}$ , and  $^{28}\text{Si}(^3\text{He}, p)^{30}\text{P}$  [These reactions will be referred to as (24-26), (26-28), and (28-30).]

The exclusion of odd-mass nuclei led to uniformity in  $Q$  values and optical-model parameters and made the DWBA calculations more reliable than in the general case. The peaks of the angular distributions for  $L=0$  and  $L=2$  transitions are expected to fall in the forward direction. It is therefore desirable to measure the proton groups at very small angles up to, say,  $120^\circ$ . Using tantalum foils to stop the direct beam it was possible to measure down to  $2^\circ$  from the beam direction.

(ii) The ratio ( $R$ ) between the measured and the calculated cross sections (at the angle of maximum cross section) was formed for each final state. The theoretical  $\mathcal{L}$  factors were obtained from rotational model wave functions.

(iii) If the ratio  $R$  is approximately constant for transitions to all final states in a particular nucleus, it is taken to indicate that the wave functions for the active nucleons were properly chosen. It was assumed that the deformation is the same for all states below 2 MeV in each particular product nucleus.

(iv) The relative size of the average value of  $R$  for each nucleus indicates the amount of core change.

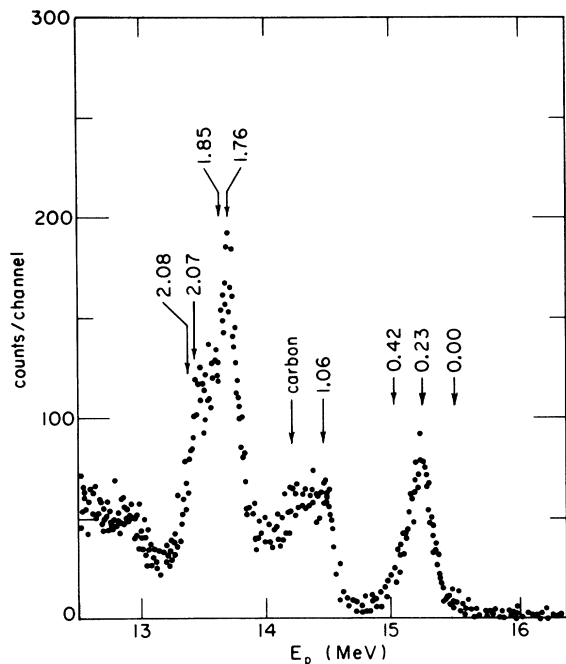


FIG. 1. Proton spectrum of the  $^{24}\text{Mg}(^3\text{He}, p)^{26}\text{Al}$  reaction at an angle of  $4^\circ$ . Thick tantalum foils were used to stop the direct beam.

The reason for this can be seen in the following argument.

In SNT reactions the rotational-model values for the spectroscopic factor are given by the well-known<sup>2</sup> expression

$$\mathcal{L} = \langle f | i \rangle^2 \mathcal{L}_0,$$

where

$$\langle f | i \rangle = \int \phi_f^*(\xi) \phi_i(\xi) d\xi. \quad (3)$$

The factor  $\langle f | i \rangle^2$  stands for the overlap of the initial and the final core wave functions and  $\mathcal{L}_0$  is the one-nucleon spectroscopic factor involving the active particle. Nilsson wave functions are normally used to calculate  $\mathcal{L}_0$ .

The spectroscopic factor in 2NT reactions is also given by Eq. (3). It is reasonable to assume that the core overlap is the same for all terms in Eq. (1); i.e., the core is the same for all active Nilsson orbits. The core overlap factor, which can be factored out, would give a reduction in the cross section proportional to  $\langle f | i \rangle^2$  which, in turn, is proportional to  $R$ .

As far as is known, there have been no attempts to determine  $\langle f | i \rangle^2$  from SNT reactions. Uncertainties in absolute DWBA calculations would prevent the determination in a single reaction and the remaining uncertainty in  $\mathcal{L}_0$  would probably be too large to make a success of the comparison technique used here. The situation is more favorable in 2NT reactions because one would, intuitively at least, expect smaller values of the core overlap factor  $\langle f | i \rangle$  because of the larger mass change between the core in the initial and the final nuclei.

Since only the changes of deformation are measured, further information is needed in order to establish absolute deformations: (i) The two members of each mass pair (i.e.,  $^{26}\text{Mg}$ - $^{26}\text{Al}$  and  $^{28}\text{Al}$ - $^{28}\text{Si}$ ) are assumed to have similar deformation; and (ii) the absolute deformations of the end-point nuclei  $^{24}\text{Mg}$  and  $^{30}\text{P}$  are either taken from measurements<sup>3</sup> (prolate deformation with  $\beta \approx +0.3$  for  $^{24}\text{Mg}$ ) or inferred from theoretical fits<sup>4</sup> to energy-level positions, etc. (weakly prolate deformation with  $\beta \approx +0.2$  for  $^{30}\text{P}$ ). In principle, this serves to fix the absolute deformation value in each nucleus involved in the chain of 2NT reactions.

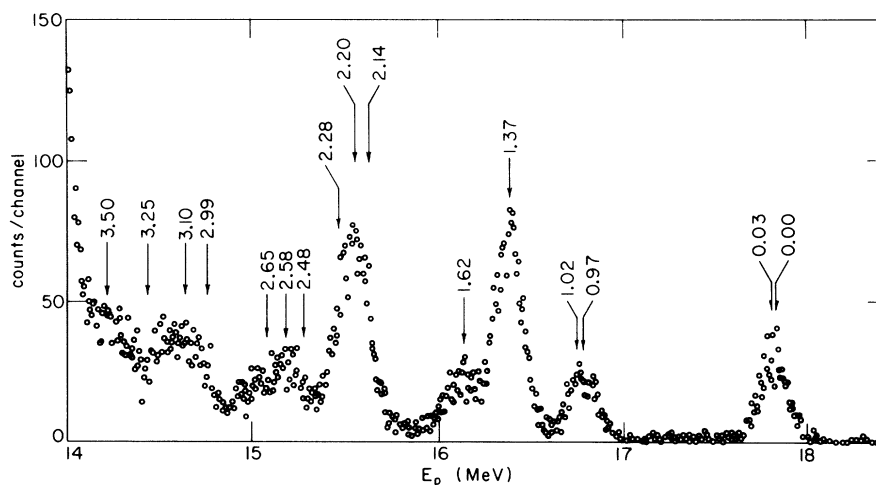


FIG. 2. Proton spectrum of the  $^{26}\text{Mg}(^3\text{He}, p)^{28}\text{Al}$  reaction at an angle of  $20^\circ$ . Thinner foils than in Fig. 1 were used.

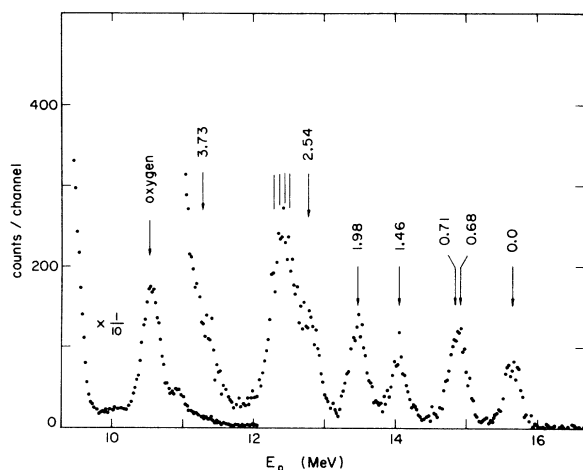


FIG. 3. Proton spectrum of the  $^{28}\text{Si}(^3\text{He}, p)^{30}\text{P}$  reaction at an angle of  $25^\circ$  using thin foils in front of the detector.

In summary, the  $(^3\text{He}, p)$  reaction will be put to twofold use: (i) to establish the applicability of the deformed rotational (i.e., Nilsson) model and (ii) to detect deformation changes. Unfortunately, part (ii) can only be done if part (i) confirms the Nilsson-model interpretation. However, there are strong indications from other data that  $^{26}, ^{28}\text{Al}$  and  $^{30}\text{P}$  are essentially rotational nuclei. The evidence for this will be reviewed in the discussion.

## 2. MEASUREMENT

A doubly charged  $^3\text{He}$  beam of 10.0-MeV energy was supplied by the Columbia University Van de Graaff accelerator. Magnesium-isotope separated targets were evaporated on thin nickel backing. The silicon target was a chip of thin self-supporting quartz glass. Proton groups with 15–19-MeV energy were produced by the  $(^3\text{He}, p)$  reactions. The groups were fully stopped in a 2-mm-thick solid-state detector, while other charged reaction

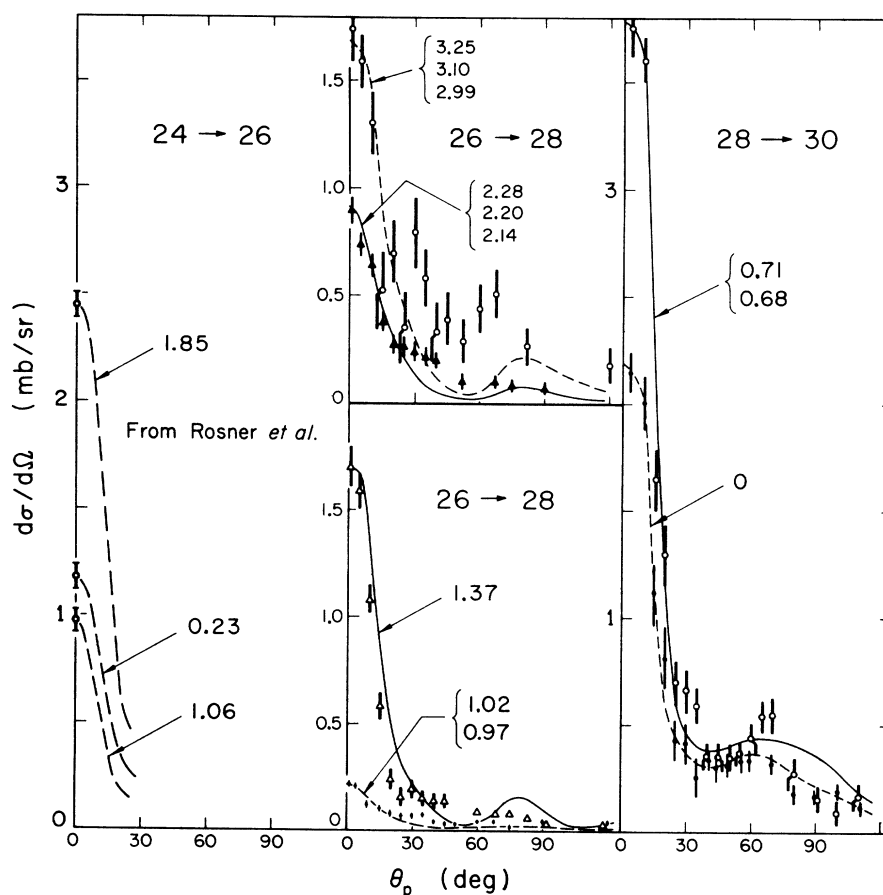


FIG. 4. Angular distribution of proton groups with  $L=0$ . The solid and the dashed lines represent the results of DWBA calculations for different final states using the same set of optical-model parameters. In the  $(24 \rightarrow 26)$  reaction only the  $\theta=0^\circ$  point was measured, since the relative angular distributions had been determined earlier by Rosner, Neogy, and Polsky (Ref. 5).

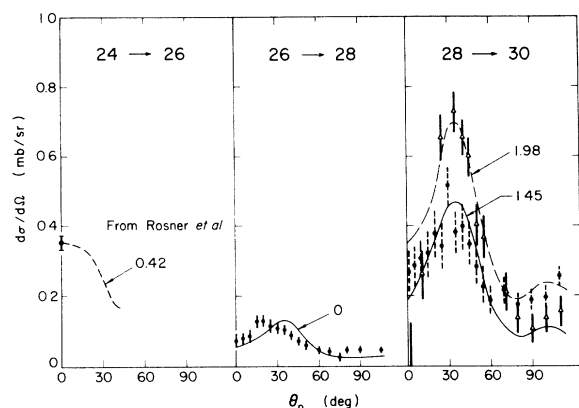


FIG. 5. The same as in Fig. 4, but for transitions with  $L=2$ .

products and the beam itself were intercepted in a tantalum foil preceding the detector. For detector angles larger than  $15^\circ$  the foil thickness could be much reduced. With the thin foils the energy resolution was 100 keV at full width at half maximum. Representative spectra are shown in Figs. 1–3 and the angular distributions are shown in Figs. 4 and 5. The angular distributions of the (24–26) reaction had previously been measured by Rosner, Neogy, and Polsky<sup>5</sup> at  $E_{\text{He}} = 12$  MeV. Therefore only the point at  $\theta = 0^\circ$  was measured assuming that the relative angular distributions are similar at  $E_{\text{He}} = 10$  MeV. Absolute differential cross sections were obtained from a comparison of the yields in

TABLE I. Rotational-model description of  $^{26}\text{Al}$ .

No.	Level in $^{26}\text{Al}$ (MeV)	$J^\pi$	$(\Omega_n, \Omega_p)$	$K$
0	0.00	$5^+$	$\frac{5}{2}, +\frac{5}{2}$	5
1	0.23	$0^+$	$\frac{5}{2}, -\frac{5}{2}$	0
2	0.42	$3^+$	$\frac{5}{2}, +\frac{1}{2}$	3
3	1.06	$1^+$	$\frac{5}{2}, -\frac{5}{2}$	0
4	1.76	$2^+$	$\frac{5}{2}, -\frac{1}{2}$	2
5	1.85	$1^+$	$\frac{1}{2}, +\frac{1}{2}$	1

the ( $^3\text{He}, p$ ) reactions and the  $^3\text{He}$  elastic scattering at  $\theta = 90^\circ$ , the latter cross sections being taken from Ref. 6. Absolute cross sections have an uncertainty of  $\pm 15\%$ . The uncertainty is less for cross sections relative to each other in the 13 transitions.

### 3. DWBA ANALYSIS

The analysis of the differential cross sections is divided into two parts: calculations of spectroscopic factors (the  $\mathcal{L}$  factors) and dynamic factors ( $B$  factors). The latter were calculated using a DWBA code (TWOPAR) developed by Bayman for 2NT. We note that:

(1) The angular distributions calculated with the TWOPAR code have the same simple stripping pat-

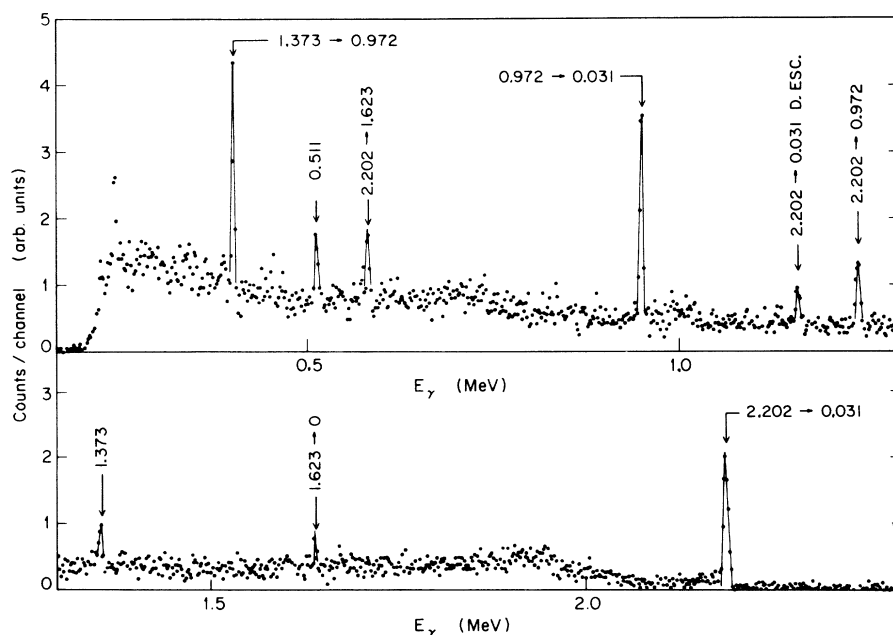


FIG. 6. The  $\gamma$ -ray spectrum in coincidence with the proton group leading to the state at 2.2 MeV excitation in the (26 $\rightarrow$ 28) reaction.

terns as the measurements (see Figs. 4 and 5). Transitions expected to have zero angular momentum transfer are peaked at  $\theta = 0^\circ$  with a half-width of  $30^\circ$ . Transitions with  $L = 2$  are peaked at  $\theta = 30^\circ$  with half-widths of  $20^\circ$  except for the transition to the excited state at 420 keV in  $^{26}\text{Al}$ . The latter transition should consequently be treated cautiously. *All other transitions are considered to proceed*

*fully via direct interaction; i.e., the DWBA analysis is applicable.*

(2) There are uncertainties in the optical-model parameters for the incident and outgoing waves, but the effects are minimized in the analysis which deals only with relative  $R$  values for an (i) intra- and (ii) inter-nuclear comparison. The optical-model values used are those of Ref. 6.

#### 4. SPECTROSCOPIC FACTORS

The spectroscopic amplitude for a  $(^3\text{He}, p)$  reaction was defined by Yoshida<sup>7</sup> as

$$\begin{aligned} \mathcal{L}_0^{1/2}(J, j_1, j_2) &= \mathcal{L}_0^{1/2}(l_1 l_2; LSJT) \\ &= \sum_{M_i} (J_i J M_i M_f - M_i | J_f M_f) \langle J_f M_f b_f | A_{J M_f - M_i}^\dagger(j_1 j_2) | J_i M_i b_i \rangle, \end{aligned}$$

where

$$A_{J M}^\dagger(j_1 j_2) = \sum_{m_i} (j_1 j_2 m_1 m_2 JM) a_{j_1 m_1 \nu}^\dagger a_{j_2 m_2 \pi}^\dagger$$

and  $a_m^\dagger$  is the creation operator for neutrons ( $\nu$ ) or protons ( $\pi$ ) in shell-model orbits. Dreizler<sup>8</sup> has derived for  $(^3\text{He}, p)$  reactions on targets with  $J_i = 0$ :

$$\begin{aligned} \mathcal{L}_0^{1/2}(J, j_1 j_2) &= \frac{2}{(2J+1)^{1/2}} \\ &\times (j_1 j_2 \Omega_1 \Omega_2 | JK) c_{j_1 \Omega_1 \nu}^{j_1} c_{j_2 \Omega_2 \pi}^{j_2} \delta_{J0}, \end{aligned} \quad (4)$$

where  $\Omega_1$  and  $\Omega_2$  are the deformed-model  $\Omega$  values for the neutron and the proton and  $c_{j\Omega}$  is the expansion coefficient of the Nilsson-model states of the active nucleons in the shell-model basis. Axial symmetry was assumed for the initial and the final nuclei and the core was assumed not to change. Protons and neutrons were treated separately as is customary in the Nilsson model. Finally,  $\mathcal{L}^{1/2} = \langle f | i \rangle \mathcal{L}_0^{1/2}$  where the factor  $\langle f | i \rangle$  is due to the deformation (polarization) of the core and the change of deformation between the target and the final states. This factor is assumed to be constant for each reaction; i.e., the deformation of the core is the same for all observed low-lying states in each individual nucleus.

### 5. RESULTS AND DISCUSSION

#### A. $(24 \rightarrow 26)$ Reaction

The available body of experimental data on  $^{26}\text{Al}$  has been reviewed and the simple axially symmetric Nilsson-model couplings of Table I have

been found to give a reasonable account of it. Only two different Nilsson orbits (Nos. 5 and 9) are required to explain all states below 2 MeV. This will be shown in the following brief review of the data.

Wasielewski and Malik<sup>4</sup> used this model, with the addition of a two-body interaction between the odd neutron and proton, to calculate the *energy spectrum*. It gave good agreement (with the exception of an inversion of the two  $J^\pi = 1^+$  levels Nos. 3 and 5 which appears to be remedied by a parameter change). Their wave functions were essentially the same as the configurations in Table I.

Experiments by Bissinger, Quin, and Chagnon<sup>9</sup> show that no state below 2 MeV has detectable  $\gamma$ -ray branchings. This is consistent with the above configuration and a result of the  $K$ - (or  $\Omega$ -) selection rule. Mixing of the two states with  $J = 1$  explains the comparatively large width of the  $1.85 \rightarrow 0.23$  decay. The absence of a transition  $1.76 \rightarrow 1.06$  follows from the  $\Omega$ -selection rule. Wasielewski and Malik<sup>4</sup> show that absolute transition rates generally agree with this model except for the  $0.42 \rightarrow 0.00$   $E2$  transition, but that, as is pointed out in Ref. 4, probably only indicates the existence of a small perturbation of axial asymmetry in the Nilsson potential.

Weidinger *et al.*<sup>10</sup> have shown that the above configurations are consistent with the results of the *single-nucleon stripping reaction*  $^{25}\text{Mg}(^3\text{He}, d)^{26}\text{Al}$ : The yields to level Nos. 0, 1, and 3 are in close agreement with theory independently of the value of the deformation (being based entirely on Nilsson orbit No. 5); the yield to No. 2 fits well for a deformation of  $\beta = 0.2 \pm 0.1$ . State No. 5 should not be accessible in this reaction. Indeed the yield is

TABLE II. Cross sections for the (24→26) reaction.

$E_x$ (MeV)	$J^\pi$	$L$	Measured peak cross section $d\sigma_m$ (mb/sr $\pm$ 20%)	$R=d\sigma_m/d\sigma_{\text{calc}}$
0.23	$0^+$	0	1.2 <sup>a</sup>	0.55
0.42	$3^+$	2	0.38 <sup>a</sup>	(0.11) <sup>b</sup>
1.06	$1^+$	0	1.0	0.51
1.85	$1^+$	0	2.5	0.51

<sup>a</sup> The double peak of transitions to the 0.23- and 0.42-MeV states were not resolved in this experiment (see Fig. 1). The ratio of yields was taken from Ref. 5.

<sup>b</sup> The reaction mechanism is not clearly understood for this level and  $R$  is uncertain.

very small and consistent with the small mixing between Nos. 3 and 5.

Weidinger *et al.*<sup>10</sup> state that the results of *single-neutron pickup* from  $^{27}\text{Al}$  [e.g. the  $^{27}\text{Al}(^3\text{He}, \alpha)^{26}\text{Al}$  reaction] is inconsistent with the model. However, it has been shown from other evidence,<sup>11</sup> that the ground state of  $^{27}\text{Al}$  contains small admixtures with  $K=\frac{1}{2}$  (and possibly  $K=\frac{3}{2}$ ) in a dominant  $K=\frac{5}{2}$  configuration. That accounts for the observed pickup transitions to state No. 2. In fact, Nurzynski, Bray, and Robson<sup>12</sup> observed no  $l=0$  component in the transition to the state at 0.42 MeV as would be expected from this model. State No. 4 was not populated at all. For the transitions to state Nos. 0 and 1 the shell model<sup>10</sup> gives the ratio ( $r$ ) of spectroscopic factors as  $r=0.09$ , while Nurzynski, Bray, and Robson<sup>12</sup> measured  $r=0.23$ . In the rotational model, these transitions involve only the  $K=\frac{5}{2}$  component in  $^{27}\text{Al}$ , and we obtain the reasonable value  $r=0.17$  (independent of  $\beta$  and admixtures in the ground state of  $^{27}\text{Al}$ ).

Since all data on  $^{26}\text{Al}$  are consistent with the Nilsson model at  $\beta=+0.15\pm 0.05$ , we adopt these wave functions to calculate the spectroscopic amplitudes in the  $^{24}\text{Mg}(^3\text{He}, p)$  reaction given in Table II. For all 2NT cross-section calculations in this section,

TABLE III.  $\gamma$  radiation coincident with  $L=0$  proton peaks.

Transition	Intensity
$2.202 \pm 0.001 \rightarrow 0.031$	$75 \pm 7$
$2.202 \rightarrow 0.973$	$19 \pm 3$
$2.202 \rightarrow 1.623$	$6 \pm 2$
Other transitions	$<3$
$3.105 \pm 0.001 \rightarrow 0.031$	$75 \pm 7$
$3.105 \rightarrow 2.202$	$25 \pm 3$
Other transitions	$<10$

TABLE IV. Rotational-model description of selected states in  $^{28}\text{Al}$ .

No.	Level in $^{28}\text{Al}$ (MeV)	$J^\pi$	$(\Omega_p, \Omega_n)$	$K$
0	0.00	$3^+$	$\frac{5}{2}, +\frac{1}{2}$	3
1	0.03	$2^+$	$\frac{5}{2}, -\frac{1}{2}$	2
2	0.97	$0^+$	$\frac{1}{2}, -\frac{1}{2}$	0
3	1.37	$1^+$	$\left\{ \begin{array}{l} \frac{1}{2}, +\frac{1}{2} \\ \frac{1}{2}, -\frac{1}{2} \end{array} \right.$	1
4	1.620	$1^+$		1
5	2.202	$1^+$	$\left\{ \begin{array}{l} \frac{1}{2}, +\frac{1}{2} \\ \frac{1}{2}, -\frac{1}{2} \end{array} \right.$	0
6	3.105	$1^+$		0

the factor  $\langle f | i \rangle$  has been set equal to 1. Deviations from this value will be discussed in Sec. 6.

#### B. (26→28) Reaction

Four transitions with large  $L=0$  components were observed. This confirms the  $J=0$  assignments to the state at 0.97 MeV initially inferred from the  $^{30}\text{Si}(d, \alpha)^{28}\text{Al}$  reaction<sup>13</sup> and  $\beta$  decay and later supported by lifetime measurements by Maher *et al.*<sup>14</sup> Due to straggling in the foils, the energy resolution was only 50 keV for the large  $L=0$  proton groups.

#### Coincident $\gamma$ Radiation in the (26→28) Reaction

In order to pinpoint these energies more accurately and to determine the  $\gamma$ -ray branchings from these states, the  $\gamma$ -ray spectrum was measured in coincidence with the proton groups with  $L=0$  at  $\theta_p=2^\circ$ . A 50-cm<sup>3</sup> Ge(Li) detector was used. The time spectrum of pulses in the proton  $\gamma$ -ray detectors was obtained in a time-to-amplitude converter. The events were stored on magnetic tape labeled with their  $\gamma$ -ray and proton energy, as well as the time pulse. The tapes were sorted off line. The spectrum in coincidence with the proton peak

TABLE V. Cross section for the (26→28) reaction.

$E_x$ (MeV)	$J^\pi$	$L$	Measured peak cross section $d\sigma_m$ (mb/sr $\pm$ 20%)	$R=d\sigma_m/d\sigma_{\text{calc}}$
0.00	$3^+$	2	0.13	0.04
0.03	$2^+$	2		
0.97	$0^+$	0	0.20	0.04
1.37	$1^+$	0	1.65	0.20
1.62	$1^+$	—	$<0.15$	
2.20	$1^+$	0	0.9	
3.10	$1^+$	0	1.1	

to the state at about 2.2 MeV is shown in Fig. 6. It proves that the level is, in fact, at  $E_x = 2.202 \pm 3$  MeV. The branching ratios are summarized in Table III. From the  $L=0$  character of the 2NT reaction these states can have either  $J^\pi = 0^+$  or  $J^\pi = 1^+$ . From the  $\gamma$  branchings  $J=0$  is excluded unless there are abnormally large  $E2$  rates. The  $J=1$  assignment to the 2.202-MeV state agrees with the measurements of Boerma and Smith<sup>15</sup> and Betts *et al.*<sup>16</sup> The  $J^\pi = 1^+$  assignment to the 3.105-MeV state is new.

#### Rotational Model in $^{28}\text{Al}$

Recently the results of an extensive shell-model calculation of  $^{28}\text{Al}$  were published.<sup>14</sup> The SNT spectroscopic factors and transition rates of some levels were well accounted for by this model, but other levels, notably those excited well in this experiment, were in worse agreement with the data. For this reason, we prefer to use rotational-model wave functions analyzing this experiment even if certain other levels could be equally well or better predicted by the shell model.

States with the configuration  $(\Omega_p, \Omega_n) = (\frac{1}{2}, \pm\frac{1}{2})$  should have the characteristics of being weakly populated in SNT reactions (i.e., via core excitations) but strongly populated in 2NT reactions (because  $L=0$  transfer). These conditions are found for the states at 0.97, 1.37, 2.20, and 3.10 MeV excitation which are therefore assumed to contain the components of the above-mentioned rotational-model configuration. Other components, such as  $(\frac{5}{2}, -\frac{3}{2})$  explain the SNT reaction spectroscopic factors, but have little influence on the cross sections of the 2NT reaction. These components enter in Eq. (1), but DWBA calculations show that  $L=0$  transfer has a much larger cross section for the transfer of  $(s_{1/2})^2$  than for transfer of  $(d_{3/2})^2$  or  $(d_{5/2})^2$ . Consequently, we neglect components

TABLE VI. Wave functions for levels in  $^{30}\text{P}$ . The arrows indicate large mixings of the wave functions.

Level in $^{30}\text{P}$ (MeV)	$J^\pi$	$(\Omega_n, \Omega_p)$	$K$
0.00	$1^+$	$\frac{1}{2}, -\frac{1}{2}$	0
0.68	$0^+$	$\frac{1}{2}, -\frac{1}{2}$	0
0.71	$1^+$	$\frac{1}{2}, +\frac{1}{2}$	1
1.46	$2^+$	$\frac{1}{2}, +\frac{1}{2}$	1
		$\frac{3}{2}, +\frac{1}{2}$	2
1.98	$3^+$	$\frac{1}{2}, +\frac{1}{2}$	1
		$\frac{1}{2}, -\frac{1}{2}$	0
		$\frac{3}{2}, +\frac{1}{2}$	2

other than  $(\frac{1}{2}, \pm\frac{1}{2})$ . The  $(\frac{1}{2}, \pm\frac{1}{2})$  coupling gives two states with  $J=1$  which we consider distributed across the four states with that spin at 1.37, 1.62, 2.20, and 3.10 MeV (see Table IV). The results of the 2NT reaction are given in Table V.

#### C. (28 → 30) Reaction

Wasielewski and Malik and Ascuitto, Bell, and Davidson<sup>4</sup> have investigated  $^{30}\text{P}$  using a rotational model with Coriolis coupling and a two-body interaction between the odd proton or neutron. A deformation of  $\beta = +0.2$  and  $+0.1$  was used. At that deformation the Nilsson level with  $\Omega = \frac{3}{2}$  is well separated from the  $\Omega = \frac{1}{2}$  level and is not included in our calculations of spectroscopic factors. The resulting rotational model interpretation is shown in Table VI. The mixings shown are those of Ref. 4. There is good agreement with level positions and  $M1$  transition rates, but some  $E2$  rates are not well predicted. These wave functions are used to calculate the 2NT cross sections of Table VII. Evidently the lowest state with  $J=3$  is inconsistent with the rotational-model interpretation.

A number of other models have been applied to  $^{30}\text{P}$ . The shell model of Glaudemans, Wiechers, and Brussard<sup>17</sup> is not capable of explaining the results of the  $(^3\text{He}, p)$  reaction. The  $R$  value for the  $J=3$  state is very large ( $R \approx 500$ ) because it has not been given a  $s_{1/2}$  component. Towner and Hardy<sup>1</sup> concluded on other grounds that this model is not suited for analysis of the (28 → 30) reaction.

A third model, the intermediate-coupling shell model of Bouten, Elliot, and Pullen<sup>18</sup> gives states with  $J^\pi = 2^+$  and  $3^+$  that contain  $s_{1/2}$  components. Unfortunately, their wave functions are not given explicitly.

A fourth model, the vibrational uniform model of Singh *et al.*<sup>19</sup> gives good predictions of many properties, but it is unlikely to yield sufficient 2NT cross section to the  $J=3$  state, since the main components of this state are based on the excitation of the core.

TABLE VII. Cross sections for the (28 → 30) reaction.

$E_x$ (MeV)	$J^\pi$	$L$	Measured peak		
			cross section $d\sigma_m$ (mb/sr)	$R = d\sigma_m/d\sigma_{\text{calc}}$ $\beta = \pm 0.1$	$\beta \approx 0.0$
0.00	$1^+$	0	2.15	0.16	0.11
0.68	$0^+$	0	} 3.75	} 0.19	} 0.13
0.71	$1^+$	0			
1.46	$2^+$	2	0.45	0.33	0.30
1.98	$3^+$	2	0.70	2 <sup>a</sup>	$\infty$

<sup>a</sup> Very sensitive to deformation.

It is apparent that the  $R$  factors in this reaction are quite large even excluding the 1.98-MeV state.

## 6. CONCLUSIONS

### A. Rotational-Model Applicability

It is established that the rotational model predicts reasonably consistent cross sections for 2NT reactions in each nucleus studied. Furthermore, the rotational-model fits are reasonably independent of the sign of deformation for moderate deformations, i.e., for  $|\beta| < 0.2$ , say. This is because:

- (i) The principal orbits involved in this mass region are Nilsson orbits No. 5 where  $c_{5/2, 5/2} = 1$  independent of  $\beta$  and No. 9 where  $c_{1/2, 1/2}$  is symmetric around the  $\beta = 0$  value and No. 8 where  $c_{3/2, 3/2} \approx 1$  with only a weak  $\beta$  dependence.
- (ii) Terms with the lowest  $l$  value dominate in the squared sum of Eq. (1); i.e., the expansion coefficient  $c_{j\Omega}$  with  $j = \Omega$  will dominate. If the  $s_{1/2}$  orbital is involved in any of the terms, one may neglect other terms.

### B. Deformation Measurements

In the calculations of the cross sections in the previous section,  $\langle f|i \rangle = 1$  was used in Eq. (3). In order to obtain over-all agreement, it is necessary to allow  $\langle f|i \rangle$  to take on three different values, one for each of the reactions (24–26), (26–28), and (28–30) in the ratio

$$\bar{R}_{24, 26} : \bar{R}_{26, 28} : \bar{R}_{28, 30} = 51 : (4 \text{ to } 20) : (16 \text{ to } 30) \\ = 1 : (0.25 \pm 0.15) : (0.45 \pm 0.15),$$

where  $\bar{R}_{24, 26}$  is the average  $R$  value for the (24–26) reactions, etc. In other words, *there is much*

*larger deformation change of the cores going from  $^{26}\text{Mg}$  to  $^{28}\text{Al}$ - $^{28}\text{Si}$  than going from  $^{24}\text{Mg}$  to  $^{26}\text{Mg}$ - $^{26}\text{Al}$  and a somewhat larger change going from  $^{28}\text{Si}$  to  $^{30}\text{P}$ .*

Knowing that the core deformation of  $^{24}\text{Mg}$  is prolate with  $\beta = +0.3$  and that  $^{30}\text{P}$  probably has  $0 < \beta \leq 0.2$  and assuming that the deformation is similar for  $^{26}\text{Mg}$  and  $^{26}\text{Al}$  and that it is similar for  $^{28}\text{Al}$  and  $^{28}\text{Si}$ , we furthermore have:

- (1) The deformation of  $^{26}\text{Mg}$ - $^{26}\text{Al}$  is prolate;
  - (2) the deformation of  $^{28}\text{Al}$ - $^{28}\text{Si}$  is oblate,
- since the deformation of  $^{28}\text{Al}$ - $^{28}\text{Si}$  cannot reasonably be more than in  $^{24}\text{Mg}$  and  $^{26}\text{Mg}$ - $^{26}\text{Al}$ .

As far as is known, there are no other published shape-sensitive measurements on  $^{26, 28}\text{Al}$  and  $^{30}\text{P}$ . Other published methods of deformation measurements can only be used on nonradioactive nuclei. One method, nucleon inelastic scattering, infers  $\beta$  from coupled-channel analysis of these cross sections, but the results have been somewhat ambiguous in the past. Rebel *et al.*<sup>20</sup> have given a summary of such measurements on  $^{28}\text{Si}$ . The most recent analyses give negative deformation, while pre-1966 papers give positive deformations. Another type of shape-sensitive measurements are based on static quadrupole measurements of the lowest  $J = 2$  state in even nuclei. Nakai, Stephens, and Diamond<sup>3</sup> gave a summary of such measurements in the  $d$ - $s$  shell. The inferred sign of the deformation parameter  $\beta$  showed a trend which is consistent with our measurements. Analysis<sup>21</sup> of the  $\gamma$  decay in  $^{28}\text{Si}$  indicates negative deformation of the isospin analog of the  $^{28}\text{Al}$  ground state in  $^{28}\text{Si}$ .

We wish to thank Dr. R. Dreizler for the derivation of Eq. (4) and for many helpful discussions. We are also very grateful to Dr. D. C. Church for helping in the experiment.

†Supported by U. S. Atomic Energy Commission.

<sup>1</sup>I. S. Towner and J. C. Hardy, *Advan. Phys.* **18**, 401 (1969).

<sup>2</sup>M. H. Macfarlane and J. B. French, *Rev. Mod. Phys.* **32**, 567 (1960).

<sup>3</sup>K. Nakai, F. S. Stephens, and R. M. Diamond, *Phys. Letters* **34B**, 389 (1971).

<sup>4</sup>P. Wasielewski and F. B. Malik, *Nucl. Phys.* **A160**, 113 (1971); R. J. Ascutto, D. A. Bell, and J. P. Davidson, *Phys. Rev.* **176**, 1323 (1968).

<sup>5</sup>B. Rosner, P. Neogy, and L. Polsky, *Phys. Letters* **27B**, 450 (1968).

<sup>6</sup>For  $^{24}\text{Mg}$ : J. L. Yntema, B. Zeidman, and R. H. Bassel, *Phys. Letters* **11**, 302 (1964); for  $^{26}\text{Mg}$ : J. Nurzynski, *Nucl. Phys.* **A141**, 257 (1970); for  $^{28}\text{Si}$ : B. H. Wildenthal and P. W. M. Glaudemans, *Nucl. Phys.* **A92**, 353 (1967).

<sup>7</sup>S. Yoshida, *Nucl. Phys.* **33**, 685 (1962).

<sup>8</sup>R. Dreizler, private communication.

<sup>9</sup>G. A. Bissinger, P. A. Quinn, and P. R. Chagnon, *Nucl. Phys.* **A115**, 33 (1968).

<sup>10</sup>A. Weidinger, R. H. Siemsen, G. C. Morrison, and B. Zeidman, *Nucl. Phys.* **A108**, 547 (1968).

<sup>11</sup>B. Lawergren, G. C. Neilson, and J. L. Honsaker, *Phys. Letters* **30B**, 470 (1969).

<sup>12</sup>J. Nurzynski, K. H. Bray, and R. A. Robson, *Nucl. Phys.* **A107**, 581 (1968).

<sup>13</sup>B. Lawergren, *Nucl. Phys.* **A96**, 49 (1967).

<sup>14</sup>J. V. Maher *et al.*, *Phys. Rev. C* **5**, 1322 (1972); J. V. Maher, H. T. Fortune, G. C. Morrison, and B. Zeidman, *ibid.*, 1313 (1972).

<sup>15</sup>D. O. Boerma and Ph. B. Smith, *Phys. Rev. C* **4**, 1211 (1971).

<sup>16</sup>R. R. Betts *et al.*, *Phys. Rev. Letters* **26**, 1121 (1971).



<sup>17</sup>P. W. M. Glaudemans, G. Wiechers, and P. J. Brusard, *Nucl. Phys.* **56**, 529, 548 (1964).

<sup>18</sup>M. C. Bouten, J. P. Elliott, and J. A. Pullen, *Nucl. Phys.* **A97**, 113 (1967).

<sup>19</sup>B. P. Singh, B. Castel, I. P. Johnstone, and K. W. C.

Stewart, *Phys. Rev. C* **5**, 1613 (1972).

<sup>20</sup>H. Rebel *et al.*, *Phys. Rev. Letters* **26**, 1190 (1971).

<sup>21</sup>B. Lawergren, I. J. Taylor, and M. Nessin, *Phys. Rev. C* **3**, 994 (1970).

PHYSICAL REVIEW C

VOLUME 6, NUMBER 6

DECEMBER 1972

## Elastic Scattering of Alpha Particles from <sup>27</sup>Al in the Energy Range 21–28 MeV\*

K. W. Kemper, A. W. Obst, and R. L. White

*Department of Physics, The Florida State University, Tallahassee, Florida 32306*

(Received 5 July 1972)

60-point angular distributions have been measured in 200-keV steps for <sup>27</sup>Al( $\alpha$ ,  $\alpha_0$ )<sup>27</sup>Al in the energy range 21–28 MeV. At an incident energy of 23.9 MeV an anomalous structure of full width at half maximum  $\sim$ 300 keV is seen for angles greater than 90°, but above 25 MeV no correlated structure is seen. The data above 25 MeV have been analyzed in terms of the optical model, and discrete potential ambiguities, as well as a radius ambiguity, have been found. These potential parameter sets were able to give qualitative fits to the data throughout the angular range 25–150° (c.m.) at the energies 24.9, 25.9, and 27.5 MeV, and at the lower energies 22.3 and 23.3 MeV the general trend of the data was reproduced.

### I. INTRODUCTION

As part of a study of  $\alpha$ -particle induced-reactions on <sup>27</sup>Al, the elastic scattering of  $\alpha$  particles by <sup>27</sup>Al has been measured in the laboratory energy range 21–28 MeV. The objective of this work was to obtain optical-model parameters for use in future distorted-wave Born-approximation calculations of the reactions under study.

Initially, it was thought this study would not be necessary, since earlier studies<sup>1</sup> indicated that  $\alpha$  scattering by <sup>27</sup>Al is direct above 17 MeV and a complete angular distribution has been measured<sup>2</sup> for  $E_\alpha = 18.82$  MeV as well as a partial angular distribution ( $\theta_{\text{lab}} < 90^\circ$ ) for  $E_\alpha = 28$  MeV.<sup>3</sup> Attempts to describe the 19-MeV data with the optical model by Srivastava and Johnson<sup>4</sup> were unsuccessful for  $\theta_{\text{c.m.}} > 80^\circ$ , where the data were higher than the calculations. An analysis of the 28-MeV data by Satchler<sup>5</sup> shows a similar feature. This result is not surprising, since for several other<sup>6</sup> *2s-1d* shell nuclei nondirect contributions to the cross section have been found to be important for angles greater than 90° in this energy range. To determine whether nondirect contributions are present at tandem energies for  $\alpha$  scattering from <sup>27</sup>Al, excitation functions and angular distributions are reported for  $\alpha$  particles of energy 21–28 MeV. The results of an optical-model analysis of the data are also presented.

### II. EXPERIMENTAL PROCEDURE

The Florida State University FN tandem Van

de Graaff was used to accelerate <sup>4</sup>He<sup>-</sup> ions and typical beam currents were 150–300 nA. The two targets used in this work were rolled foils whose thicknesses were 200 and 50 keV for 25-MeV  $\alpha$  particles. Since the <sup>197</sup>Au( $\alpha$ ,  $\alpha_0$ )<sup>197</sup>Au excitation function does not exhibit any radical fluctuations in the energy range covered here<sup>7</sup> a flash of gold evaporated on the targets was used to provide a continuous system check. The detector solid angles were determined by scattering 6-MeV  $\alpha$  particles from a gold target whose thickness was determined by the energy loss of  $\alpha$  particles from an <sup>241</sup>Am source.

Differential cross sections were measured at 16 angles simultaneously with Si-surface-barrier detectors mounted in a ring which was contained in a 45-cm scattering chamber.<sup>8</sup> The data were accumulated in a TMC 4096-channel analyzer coupled to an EMR-6130 computer for on-line data analysis. By adjustment of the beam current, the dead time of the analyzer was kept to less than 10%.

The systematic error in the data estimated from the reproducibility of the data obtained in different runs is 3% and is due to uncertainties in the beam-current integration and the solid-angle determinations. The statistical uncertainty was always less than 3% and the absolute error assigned to each data point was between 4 and 5%.

### III. EXPERIMENTAL RESULTS

The data reported here consist of excitation functions in the bombarding energy range from